Publisher: GSA
Journal: GEOL: Geology
Article ID: Template

DR. DANIEL M GRIFFITH (Orcid ID : 0000-0001-7463-4004)

Article type : Research Paper

Paper Type: Original Article

Title: **Multi-century stasis in C_3 and C_4 grass distributions across the contiguous United States since the industrial revolution**

Daniel M. Griffith[1], Jennifer M. Cotton[2], Rebecca L. Powell[3], Nathan D. Sheldon[4], and Christopher J. Still[1]

[1]*Forest Ecosystems and Society, Oregon State University, Corvallis, Oregon, U.S.A.*

[2]*Department of Geological Sciences, California State University Northridge, Northridge, California, U.S.A.*

[3]*Department of Geography and the Environment, University of Denver, Denver, Colorado, U.S.A.*

[4]*Department of Earth and Environmental Sciences, University of Michigan, Ann Arbor, Michigan, U.S.A.*

Corresponding author:
Daniel M. Griffith; T: +1(910)5450632; E: daniel.griffith@oregonstate.edu

Running header: **Multi-century stasis in C_3/C_4 distributions**

Word Count: 6802

ABSTRACT (300)

Aims Understanding the functional response of ecosystems to past global change is crucial to predicting performance in future environments. One sensitive and functionally significant attribute of grassland ecosystems is the percentage of species that use the C_4 versus C_3 photosynthetic pathway. Grasses using C_3 and C_4 pathways are expected to have different responses to many aspects of anthropogenic environmental change that have followed the industrial revolution, including increases in temperature and atmospheric CO_2, changes to land management and fire-regimes, precipitation seasonality, and nitrogen deposition. In spite of dramatic environmental changes over the past 300 years, it is unknown if the C_4 grass percentage in grasslands has shifted.

Location Contiguous United States of America

Methods Here, we used stable carbon isotope data (i.e., $\delta^{13}C$) from 30 years of soil samples, as well as herbivore tissues that date to 1739 CE, to reconstruct coarse-grain C_3 and C_4 grass composition in North American grassland sites to compare with modern vegetation. We spatially resampled these three datasets to a shared 100-km grid, allowing comparison of $\delta^{13}C$ values at a resolution and extent common for climate model outputs and biogeographic studies.

Results At this spatial grain, the bison tissue proxy was superior to the soil proxy because the soils reflect integration of local carbon inputs, whereas bison sample vegetation across landscapes. Bison isotope values indicate that historical grassland photosynthetic-type composition was similar to modern vegetation.

Main conclusions Despite major environmental change, comparing modern plot vegetation data to three centuries of bison $\delta^{13}C$ data revealed that the biogeographic distribution of C_3 and C_4 grasses has not changed significantly since the 1700s. This is particularly surprising given the expected CO_2 fertilization of C_3 grasses. Our findings highlight the critical importance of capturing the full range of physiological, ecological and demographic processes in biosphere models predicting future climates and ecosystems.

Keywords: bison, C_4 photosynthesis, environmental change, grass, grassland biogeography, North America, spatial scale, vegetation stasis, $\delta^{13}C$

INTRODUCTION

Industrialization in the 18th century intensified human modification of ecosystems, and understanding the resulting impacts on ecosystem functioning and vegetation distributions has become a principal goal of ecologists. A key functional attribute of grassland ecosystems that should be sensitive to environmental change is the percentage of grasses that use the C_4 photosynthetic pathway versus the C_3 ancestral pathway. For example, C_4 grasses, which are adapted to warm and open-habitats, should be favored by increasing temperatures whereas C_3 grasses should be favored under elevated CO_2 (Ehleringer et al., 1997)—a balance with potential consequences for vegetation structure and fire regimes globally (Bond & Midgley, 2012). C_3 and C_4 vegetation also differ fundamentally in their nitrogen and water use efficiencies, with potential consequences for their competitive dynamics (Tilman & Wedin, 1991; Long, 1999) and palatability to herbivores (Heckathorn et al., 1999). In 2015, surface temperatures on Earth were 1 ºC above preindustrial levels and the average global CO_2 concentration reached 399.4 ppm – roughly 120 ppm above preindustrial levels (Blunden & Arndt, 2016). Concurrently, atmospheric nitrogen deposition has drastically increased (Vitousek et al., 1997), trophic structure has shifted (e.g., Ripple et al., 2015), land management practices have changed radically and fire regimes may have been suppressed (Ramankutty & Foley, 1999; but see Power et al, 2008). Although post-industrial changes in the percentage of C_4 versus C_3 grasses should have important consequences for ecosystem functioning at a range of spatial-grains (Still et al., 2003), there have not been assessments of photosynthetic pathway representation over the last several hundred years at regional extents despite the use of vegetation proxies over deeper geologic time.

Stable carbon isotope data (i.e., $\delta^{13}C$ [VPDB]) from soils and herbivore tissues are widely used as proxies of ecological properties and processes such as the relative abundance of C_3 and C_4 plants, water use efficiency in C_3 plants, productivity, trophic position, aridity, and tree cover (e.g., Dawson et al., 2002; Still et al., 2003; Kohn, 2010; Diefendorf et al., 2010; Cerling et al., 2011; Ladd et al., 2014). Yet, $\delta^{13}C$ values from such proxies have only rarely been compared directly to abundances of C_3 and C_4 source vegetation at the spatial resolution and extent of many biogeographic processes (e.g., C_4 range expansion; Wynn et al., 2006; Jenkins & Ricklefs, 2011; Strömberg, 2011; Powell et al., 2012; Chen et al., 2015). Similarly, applications that depend on $\delta^{13}C$ data often fail to consider the spatial grain at which different $\delta^{13}C$ proxies integrate C (Auerswald et al., 2009). For example, the $\delta^{13}C$ composition of soil surface layers is

related to soil texture and organic matter over relatively small areas (~m^2; Wynn et al., 2006; Bai et al., 2012; Liang et al., 2016), while herbivore tissues correspond to vegetation composition over larger spatial extents (~10s of km2; Meagher, 1989; Kohn & Fremd, 2008; Auerswald et al., 2009; Widga et al., 2010). As a result, the spatial scale of C integration may impact how well $\delta^{13}C$ proxies represent vegetation at the spatial extents and spatial grains that they are often used. In order to draw robust inferences about vegetation change at a regional scale, we compare both soil and animal proxies to vegetation plots across the same geographic extent.

The primary driver of naturally occurring terrestrial variation in $\delta^{13}C$ is the difference in isotope discrimination between plants that use either the C_3 or C_4 photosynthetic pathway (Farquhar et al., 1989). C_4 photosynthesis results in minor atmosphere-plant tissue fractionation (-3 to -5‰). This fractionation is relatively consistent across >20 independent C_4 grass lineages and across C_4 subtypes (i.e., 1‰ difference between NADP-me and PCK/NAD-me) (Ehleringer et al., 1997; Cerling & Harris, 1999; Long, 1999; Sage et al., 2011; Grass Phylogeny Working Group II, 2012). The ancestral C_3 photosynthetic pathway has larger and more variable atmosphere-plant tissue fractionation, especially for woody plants. Beyond the differences between C_3 and C_4 carbon isotope discrimination, there is considerable variation in plant $\delta^{13}C$ among C_3 plants that relates to environmental variation. For example, trees are almost exclusively C_3 (Sage & Sultmanis, 2016) but their $\delta^{13}C$ values can vary widely with plant physiology/morphology, biome, along environmental gradients (i.e., with mean annual precipitation [MAP])(Kaplan et al., 2002; Kohn, 2010; Diefendorf et al., 2010; Ladd et al., 2014), and in lock step with long-term changes to the $\delta^{13}C$ value of the atmosphere. In general, the present-day $\delta^{13}C$ value for C_4 grasses centers around -12.5 (± 1.1‰) while C_3 grasses have a mean of -26.7 (± 2.3‰)(Cerling et al., 1997), although the data come from arid environments, which would bias the results toward more positive values (Kohn, 2010).

Palaeoecological, palaeoclimatological, and modern carbon cycling applications using $\delta^{13}C$ that rely on measurements from soils and palaeosols must account for changes to isotopic ratios due to plant biomass allocation patterns, atmospheric $\delta^{13}C$ change, litter decomposition, preservation, diagenesis, and numerous other processes (Ehleringer et al., 2000; Passey et al., 2002; Fox & Koch, 2003; Wynn & Bird, 2007; Bowling et al., 2008; Tipple et al., 2010; Angelo & Pau,

2015). In addition, each of these various processes has inherent spatial and temporal ranges over which they influence the integration of C (e.g., Bowen, 2010). For example, surface soils (i.e., 0–5 cm depth) might reflect 10s to 100s of years of soil carbon turnover and may be largely influenced by carbon assimilated at spatial extents on the order of metres (Leavitt et al., 2007; Bai et al., 2012). Since remotely sensed vegetation data are represented at resolutions of 100s of metres (e.g., 250 m to 1 km grids in MODIS), grain size differences may contribute to poor alignment with soil proxies reported in the literature. For example, Ladd et al. (2014) show that leaf area index (LAI) measured *in situ* can be represented well by soil $\delta^{13}C$ across many ecosystems, but that remotely sensed LAI at 1 km is poorly correlated with soil $\delta^{13}C$.

In contrast to soils, $\delta^{13}C$ in herbivore tissues reflects diet composition (accounting for fractionation) over restricted life spans (or developmental periods), but potentially represent forage selection across an entire home range or migratory route (Meagher, 1989; Widga, 2010). Therefore, animal $\delta^{13}C$ values will usually integrate C from a larger surface area than soils, and the temporal and spatial extents at which C is integrated are likely to be species (and tissue) specific depending on the ecology of the herbivore. For example, American bison (*Bison bison* **[***Linnaeus, 1758];* hereafter bison) live ~15 years and their tissues represent $\delta^{13}C$ from grazing over large spatial extents such as an entire ecosystems or migration circuits. The period of time recorded by $\delta^{13}C$ in animals is tissue-specific, varying from continuous for hair (Ayliffe et al., 2004) to ~1 year for enamel (Gadbury et al., 2000) and multiple years for bone (Tieszen, 1994). Because the stable isotope composition of animal tissues reflects their dietary inputs, studies often use $\delta^{13}C$ data and other stable isotopes to determine the feeding sites or origins of migrating animals such as birds (Hobson et al., 2012), bats (Segers & Broders, 2015), fish (MacKenzie et al., 2011), and others (Hobson, 1999). These location assignments depend on "isoscapes," or spatially continuous representations of the distribution of isotope signatures (Bowen, 2010; Powell et al., 2012), which are themselves produced from datasets with different spatial grains, such as modeled vegetation composition and interpolated climate data in the case of some stable carbon isoscapes. Carbon isotopes from fossilized animal tissues are also used to reconstruct past climate and vegetation conditions, for example in investigating the Miocene rise to dominance of C_4 grasses in open habitats (Cerling et al. 1997; Passey et al., 2002; Fox & Koch, 2003; Strömberg, 2011).

Given the importance of carbon isotope patterns to such a wide range of applications and fields, the goals of this study were twofold: first to evaluate common $\delta^{13}C$ proxies for their ability to represent vegetation at the temporal and spatial extents relevant to post-industrial revolution environmental change, and second, to investigate the magnitude of change in C_3 and C_4 grass relative abundances in the conterminous USA over the last 300 years. We adopted a coarse-grain approach so that the analysis corresponds better to the scale (i.e., spatial grain and extent) of Earth System Models, and to many palaeoclimatological and location-assignment studies (e.g., 100 km). We emphasize the importance of examining the performance of our proxy data at this coarse resolution because scaling is often complex (Goodchild, 2011) and there is an extensive body of literature that extrapolate point measurements of isotope values to large spatial and temporal extents (reviewed in: Hobson, 1999; Dawson et al., 2002; Bowen, 2010; Beerling & Royer, 2011; Strömberg, 2011). To assess the relationships between $\delta^{13}C$ proxies and vegetation composition, we combined three multi-source datasets from North America: (1) herbaceous C_3 and C_4 grass relative abundances from vegetation plots, (2) surface soil $\delta^{13}C$ measurements, and (3) herbivore tissue $\delta^{13}C$ measurements. Finally, we examined differences between $\delta^{13}C$ proxies and modern vegetation through time in order to detect vegetation change occurring over last 300 years.

MATERIALS AND METHODS

Bison $\delta^{13}C$, soil $\delta^{13}C$, and plot-level estimates of grass relative abundance are each multisource datasets assembled from the literature (Supplemental Methods). Vegetation cover-abundance data come from plots (<1000 m^2) that sampled grass-dominated herbaceous strata to the species level, regardless of the presence of other strata such as trees (Griffith et al., 2015). The plot data were not originally restricted to grasslands; however, in this study we used only grassland plots as the soils come from grassland sites. The dataset includes roughly 40,000 plots collected in the last 40 years. We chose to represent the relative cover abundance of grasses using different photosynthetic pathways (i.e., C_3 versus C_4) using a single metric based on the percent of grasses that use the C_4 pathway. Grass species were classified as C_3 or C_4 according to Osborne et al. (2014) and a metric of relative percent C_4 abundance called "C_4 Cover (%)" was calculated by dividing the C_4 absolute abundance by the sum of C_4 and C_3 grass absolute abundances. Some of

the dominant C_4 species included *Andropogon gerardii*, *Bouteloua gracilis* and *Schizachyrium scoparium*, whereas C_3 dominants included, for example, *Poa pratensis* and species from *Festuca* and *Agropyron*. We used the C_4 grass percentage, rather than the entire herbaceous fraction, because the plots are grass dominated, C_4/C_3 assignments are readily available for grasses, grass areal cover represents standing biomass well, and to maintain consistency with previous studies that focus on grasses (e.g., Hoppe et al. 2006). The raw bison $\delta^{13}C$ data include 281 separate samples of collagen, hair, enamel, or horn sheaths from modern and historical bison (<300 yr; 48 unique sites) and are adjusted to represent the $\delta^{13}C$ of the animal's diet by correcting for tissue-dependent fractionation and for industrial modification to atmospheric $\delta^{13}C$ (preindustrial $\delta^{13}C$ = -6.3 ‰; Friedli et al., 1986). As such, our modern and historical bison $\delta^{13}C$ data were corrected to reflect preindustrial values, instead of modern atmospheric $\delta^{13}C$ which is continually changing. Bison samples come from unplowed, non-agricultural lands. Soil $\delta^{13}C$ data come from 262 new and literature derived measurements of surface organic C samples (single cores to 5 cm depth), collected within the last 30 years and therefore representing C integration over the last <100 years depending on residence times (Leavitt et al., 2007). The soils have not been tilled recently or had fertilizers added. New surface soil samples were analysed following the methods of (Cotton & Sheldon, 2012) and details are reported in Supporting Information.

To facilitate the comparison of these independent datasets, the data were resampled onto common raster grids of varying grain sizes, evaluating grid dimensions of 5, 10, 50, 100, and 200 km. We adopted a grain size of 100 km because this resolution offered the maximum number of grid cells containing isotope data (i.e., either soil or bison samples) while preventing large grid cells with very distant isotope and corresponding plot data (i.e., within grid cells nearest neighbour distances between isotope and plot data were kept below around 10 km; Fig. S1 in Appendix S1). This process resulted in 38 grid cells with both soil and plot data, and 18 grid cells that contain both bison and plot data (Fig. 1). When aggregating raw data to the grid, each cell was assigned the mean of all overlaying point data as its value (mean number of samples per grid cell ± SE was 138.9 ± 21.0, 3.1 ± 0.5, and 7.6 ± 3.5 for plots, soils, and bison, respectively). We considered weighting the mean values by distance, but we proceeded with the simple mean because inverse-distance weighting for the bison grid cell with the largest range of sample-to-centroid distances only changed the value by 0.1 ‰. While this approach allows for the

comparison of these datasets, it must rely on the assumption that grassland composition is uniform within grid cells and that the values apply only to grassland portions of cells. Gridding the data therefore produces another source of error that can contribute to misalignment of proxies and vegetation because point measurements now represent larger areas.

We assembled several additional environmental and ecological datasets representing factors that might influence the isotopic composition of surface soil and herbivore tissue. Mean annual temperature (MAT) and mean annual precipitation (MAP) were extracted from the PRISM Climate Group 30-year climate normal dataset for 1971–2000 (http://www.prism.oregonstate.edu/; 800 m resolution). Summer precipitation (SP) was calculated from PRISM monthly data. For each bison sample, data on atmospheric CO_2 concentrations were obtained based on sample date from Keeling et al. (2005) and from Friedli et al. (1986), whereas paleo-atmospheric CO_2 data come from Lüthi et al. (2008). Additional soil data including organic carbon (OC %) and clay (%) were obtained from the Harmonized World Soil Database (Nachtergaele & Batjes, 2012). Tree cover and other non-herbaceous strata were not sampled in a consistent manner in vegetation plots so we used the percent tree cover dataset from (Sexton et al., 2013)(30 m resolution). The percentage of grasses that were C_3 invaders in the vegetation plot dataset was also calculated from the vegetation plot inventory (Griffith et al., 2015). Ladd et al. (2014) suggest that leaf area index (LAI) correlates well with soil $\delta^{13}C$ across ecosystems because it reflects water use, but LAI showed very little variation among all grid cells and was therefore not included. All additional environmental/vegetation data were resampled onto the same grid as the isotope data as a simple mean.

Data analysis began by fitting separate weighted least squares regression models relating source vegetation (i.e., C_4 Cover %) to the resulting soil $\delta^{13}C$ and bison $\delta^{13}C$ values from the 100 km grid (Fig. 2). The isotope data were weighted inversely proportional to their errors using the lm() function in the statistical computing environment R (R Development Core Team, 2012). To assess whether additional variation in $\delta^{13}C$ values could be explained by factors other than C_4 Cover %, we developed structural equation models (SEMs) that allowed us to disentangle the direct effects of variables on $\delta^{13}C$ from indirect effects on $\delta^{13}C$ that were mediated by their effects on vegetation composition (C_4 cover). In essence, SEM can be conceptualized as a

network of interconnected linear regressions (i.e., some response variables are themselves predictor variables) that are fit simultaneously, often with the goal of distinguishing direct and indirect causal relationships. The individual paths, or causal links, have standardized effect sizes that can be interpreted similarly to correlation coefficients (Grace et al., 2010). We constructed separate *a priori* models for soil (Fig. 3a) and bison (Fig. 3a) $\delta^{13}C$ values that specified all causal relationships (paths in Fig. 3) among variables. Climate variables are expected to have indirect effects on both soil and bison $\delta^{13}C$, mediated through their influence on C_4 plant distributions. However, climate might also have direct influences on isotopic values due to effects on microbes, metabolism, plant biomass allocation, or other processes influencing C integration (e.g., Angelo & Pau, 2015).

Many studies have demonstrated that the seasonal distribution of rainfall and temperature are important drivers of C_4 and C_3 vegetation (Teeri & Stowe, 1976; Winslow et al., 2003; Griffith et al., 2015). We used MAT and SP as potential climatic predictors of C_4 abundance. Our primary goal was to describe any variation in $\delta^{13}C$ that was not driven directly by C_4 abundance (e.g., variable fractionation related to MAP; Diefendorf et al., 2010; Kohn 2010). In the case of the bison data, we also account for temporal variation in CO_2, but did so by relating CO_2 directly to $\delta^{13}C$ because there is limited temporal variation in the vegetation plots (Collatz et al., 1998; Kohn & McKay 2012). Paths from tree cover and soils to $\delta^{13}C$ were not included in the bison SEM as they are not expected to have any direct links to grazer tissue composition (i.e., they should be absent from their diets). We included C_3 invasives as a predictor of C_4 abundance because the presence of C_3 invasive grasses reduces C_4 abundance below climate expectations (Griffith et al., 2015) and some invasives have been present for long enough to be reflected in bison diets (Grace et al., 2000). These models were fit to data using the sem() function in the R package 'lavaan' (Rosseel, 2012) and model fit was assessed following Grace et al. (2010)(see Supplemental Methods)(Fig. 4).

We applied equation 1 from Kohn (2010) to predict theoretical $\delta^{13}C$ C_3-endmember values for modern and historical bison samples to explicitly account for $\delta^{13}C$ variability in the C_3 endmember (Diefendorf et al. 2010; Kohn 2010). The predicted end members had a mean of -26.7 ± 0.14 SE and a range of -25.4 to -27.9. Variation in these theoretical C_3-endmembers was

not associated with bison diet $\delta^{13}C$ (or with residuals after accounting for actual C_4 grass abundance) (Pearson's correlation, $p > 0.05$). We inspected the three most negative bison $\delta^{13}C$ values, which had measurements of -26.85, -26.44, and -26.23 ‰ after converting the data from preindustrial to modern to values (Fig. S2). For these three samples, the predicted C_3 endmember values using equation 1 from Kohn (2010) were 0.38, 0.17, and 0.32 ‰ more negative than our measurements, respectively.

Finally, to explore potential differences between the spatial variability of soil $\delta^{13}C$ and bison $\delta^{13}C$ data, we fit spherical semivariograms to each dataset, including the plot-level C_4 cover % for reference. A semivariogram is a geostatistical function that describes variability of a given parameter over different spatial ranges (lag distances). The parameters from fitted theoretical semivariograms describe important spatial features of a dataset, such as the "sill," which describes the total variation of the variable, and the "nugget," which describes unexplained fine-scale variation (see Supplemental Methods)(Table 1). We focus on the nugget-to-sill ratio, which is a measure of the spatial variation that exists below our 100 km grid cells as well as non-spatial measurement error. This metric is important because it is a quantitative estimate of variation at local scales (i.e., < grid resolution) and provides a test of the hypothesis that there are scale differences among $\delta^{13}C$ proxies that could influence how well they perform at coarse grain sizes. Semivariograms were fit with the fit.variogram() function in the R package 'gstat' (Table 1) using the entire grid-aggregated $\delta^{13}C$ proxy and vegetation plot data from across the conterminous USA.

Following the assessment of soil and bison isotopic proxies, vegetation change over the last 300 years was investigated by comparing bison $\delta^{13}C$ data from three time slices to modern C_4 distributions. To do so, bison data were organized into three temporal categories: "modern" samples (last 50 years), "historical" samples (51 – 300 years ago), and a third, "fossil" dataset was obtained from Cotton et al. (2016) dating to the last glacial maximum were included as a reference for the magnitude of geologic vegetation change. The modern (n = 17) and historical (n = 16) data subsets were a representative sample of the full bison dataset, both spatially and in terms of diet $\delta^{13}C$ (Fig. S5). We fit a weighted least squares regression with the modern bison $\delta^{13}C$ as the dependent and C_4 % from plots as the independent variable, and then used this

calibration model to predict the expected $\delta^{13}C$ of the historical and fossil data. The residuals (the observed – predicted) from this model were calculated for the modern, historical, and fossil datasets. This was used to represent differences from modern vegetation by relating the residuals from this relationship to the number of years before present with a Generalized Additive Model (GAM) (Fig. 5; using the R package 'mgcv'; Wood & Wood, 2016).

RESULTS

The linear model relating bison $\delta^{13}C$ to source vegetation performed very well (Fig. 2; 88% variance explanation, regardless of regression weighting), whereas soil $\delta^{13}C$ was only weakly related to source vegetation at a resolution of 100 km (Fig. 2; 42%, and only 21% in a simple linear model). We considered the possibility that a source of error in the soil relationship could be due to the presence of non-grass herbaceous vegetation; however, a re-analysis of soil $\delta^{13}C$ with the C_4 percentage of the entire herbaceous layer (assuming all forbs to be C_3) resulted in a slightly reduced variance explanation (18%). Both the bison and soil datasets had similar ranges of $\delta^{13}C$ values, representing expected source vegetation ranging from completely C_3- to completely C_4- dominated sites (Fig. S2 in Appendix S1). Variation in bison $\delta^{13}C$ was associated with variation in modern vegetation abundance, even for samples up to 300 years old (Fig. 5; Cotton et al., 2016) and the calibration regression model fit only to modern bison samples was strong ($r^2 = 0.89$).

Structural equation models were fit in order to assess the direct effects of environmental and biogeographic variation on soil and bison isotope values beyond their indirect controls on C_4 versus C_3 vegetation (see Methods). Previous independent analyses for the raw bison (Cotton et al., 2016) and vegetation plot (Griffith et al., 2015) datasets suggest that C_3 and C_4 vegetation abundances can be predicted by the crossover temperature (COT) model. COT is a compound variable that consists of a count of months per year that climatically favor C_4 vegetation (e.g., monthly mean >22 °C and >25 mm rainfall and assuming modern CO_2 concentrations; Collatz et al., 1998; Still et al., 2003). However, we used MAT, SP, and CO_2 instead of COT so that it was possible to parse out any direct and indirect influences of each climate variable on $\delta^{13}C$ values independently (see methods; Fig. S3 and S4 in Appendix S1). Additional explanatory variables increase the explained variance (values from simple lineage models used for comparison to

SEM) for both soil (from 21 to 28%) and bison (from 88 to 92%) $\delta^{13}C$ (Fig. 4). For soils, this increase is due mostly to the incorporation of tree cover because of a direct influence (as a carbon source) on $\delta^{13}C$ of soil organic matter and the reduction in C_4 abundance due to tree cover (which indirectly modifies $\delta^{13}C$). For both soil and bison, precipitation had a direct, positive effect on $\delta^{13}C$. The environmental controls on C_4 relative abundance were consistent between the two models and similar to the analysis of the raw vegetation plot data (Griffith et al., 2015).

Each dataset (soil, bison, and vegetation plot) independently captures the latitudinal gradient in vegetation C_4 % cover across the Great Plains of North America (Teeri & Stowe, 1976; Paruelo & Lauenroth, 1996), yet the semi-variogram revealed unique spatial patterns in each dataset (Table 1). Most notably, the datasets differed in the degree of heterogeneity that exists at a spatial range smaller than our grid dimensions (i.e., <100km), as represented by the nugget-to-sill ratio. There was an intermediate amount of unexplained local variation (19%) in C_4-cover data, consisting of measurement error and variation at distances less than 100 km. In contrast, soil $\delta^{13}C$ had more (31%) and bison $\delta^{13}C$ had less (8%) variation that was not explained by autocorrelation.

Finally, our exploration of deviations in C_3 and C_4 grass relative abundances over time revealed, that for the previous 300 years, photosynthetic representation has been similar to modern conditions (Fig. 5). This result is demonstrated by the overlap of the 95 % confidence interval from our GAM with a residual of zero (horizontal zero line in Fig. 5) for all times prior to 300 year BP.

DISCUSSION

Across the Great Plains in the conterminous United States, coarse-grain variation in the percentage of grasses that use the C_4 photosynthetic pathway has changed little in the last 300 years (Fig. 5). Most surprising is the complete lack of a CO_2 fertilization for C_3 grasses expected based on physiology (Collatz et al., 1998), suggesting that there are complicating factors that are buffering this response in grassland ecosystems (Morgan et al., 2011). This stasis in vegetation

distributions is unexpected from both biogeographic and ecophysiological perspectives, given the drastic changes to the environment that have occurred during this time period (Blunden & Arndt, 2016). Global atmospheric CO_2 concentrations and surface temperatures, factors directly influencing the physiology of C_3 versus C_4 plants (Ehleringer et al., 1997), have rapidly increased over the last 300 years to the highest levels since before the appearance of the genus *Homo*. Furthermore, nitrogen deposition has increased, fire regimes may have been reduced, and land management has changed drastically—all factors expected to have large, differential impacts on C_3 versus C_4 grasses (Tilman & Wedin, 1991; Long, 1999; Ramankutty & Foley, 1999). Despite these changes, the distribution of grass photosynthetic types appears to be broadly unchanged in grassland sites.

This result is highly relevant to both Miocene C_4 range expansions as well projections for near-future global change. Physiologically, a 1 ºC increase in temperature should have only a small impact on C_4 versus C_3 photosynthesis, but the insensitivity of C_4 distributions to a 143 % increase in CO_2 is particularly striking (Ehleringer et al., 1997). This result mirrors the findings of (Cotton et al., 2016) that C_4 grasses expanded northward despite rising CO_2 since the Last Glacial Maximum (LGM) and that most CO_2-driven (post-glacial) increase in C_3 grasses has occurred at concentrations below 280 ppm, although some change is still expected (Collatz et al., 1998; Cotton et al., 2016). Similarly, reduced fire frequencies due to human activities has not favored C_3 grasses broadly across the C_4 sites. In contrast, the Miocene rise to ecological dominance of C_4 grasses occurred largely during times of little CO_2 or temperature change (Beerling & Royer, 2011), with changes to precipitation seasonality and consequences for fire frequency being the most likely drivers (Scheiter et al., 2012; Cotton et al., 2016). Therefore, it is unclear what mechanisms have reinforced photosynthetic type composition since the industrial revolution. As this study focuses on grass only, it also provides a useful comparison to work focusing on CO_2 enrichment effects on C_4 grasses versus C_3 woody vegetation, a contrast that is potentially more sensitive to CO_2 change and interactions with fire and precipitation regimes in tropical regions (Bond & Midgley, 2012).

Using spatially coarse-grain data, the relative composition of C_3 and C_4-grass from vegetation plot inventories was better correlated with bison than soil $\delta^{13}C$. Furthermore, the relationship

between bison and vegetation composition was surprisingly strong given that the bison tissues date across the last 300 years (Fig. 5), but plot data are from only the last 40 years (44% of the modern bison data are older than 40 yrs). Conversely, the vegetation-soil $\delta^{13}C$ relationship was surprisingly weak (Fig. 2). Previous studies have found strong positive relationships between soil and herbivore $\delta^{13}C$ and vegetation composition. For the study extent (the conterminous USA) these studies include Great Plains soil $\delta^{13}C$ with modeled C_4 vegetation percentage (von Fischer et al., 2008) and bison $\delta^{13}C$ with nearby (<40 km) vegetation plots (Hoppe et al., 2006). In this study, we find a much weaker relationship than von Fischer et al. (2008) for soil $\delta^{13}C$ when compared to standing vegetation. To our knowledge, this is the first study that compares soil and bison $\delta^{13}C$ proxies to measured vegetation composition at a consistent, coarse spatial grain over a broad spatial extent. Thus, this study offers a key assessment of the impact of the differing spatial resolutions of processes, such as C integration in herbivores versus soils, on their representation in biogeographical- and palaeo-$\delta^{13}C$ datasets. Although the scale difference between proxies from herbivore tissues and collections of soil points is intuitive, we stress that it is commonplace in the literature to apply local soil measurements across large spatial and temporal extents (as reviewed in: Hobson, 1999; Dawson et al., 2002; Bowen, 2010; Beerling & Royer, 2011; Strömberg, 2011). The superior performance of herbivore proxies compared to soils in this study suggests that other grazer and browser vegetation proxies, especially those with longer fossil records like camels or deer, may also perform well (barring the effects of diet preference)—as such, conducting similar studies in such species would represent a significant step forward.

Soil $\delta^{13}C$ was linearly related to relative abundance of C_4 grasses, but the relationship was also improved by the addition of tree cover and MAP as direct predictors of $\delta^{13}C$ in our SEM (Fig. 4). Tree cover had a negative relationship to soil $\delta^{13}C$ values, likely reflecting trees as an isotopically depleted (C_3) carbon source, a finding that mirrors the woody cover relationship used by (Cerling et al., 2011). Our vegetation plots are located in grass-dominated areas and 98% of the grid cells contained mean LAI values <1 as observed with MODIS LAI (i.e., they are grassland plots)(Asner et al., 2003). As such, comparing local- and ecosystem-level variation in $\delta^{13}C$ proxies might also be valuable for studies that examine $\delta^{13}C$ across broader LAI gradients (similar to Ladd et al., 2014) or for combination with phytolith data for improving palaeo-LAI

proxies (Dunn et al., 2015). The SEM path from MAP to soil $\delta^{13}C$ was positive, and harder to explain than the other paths because rainfall is expected to increase carbon isotope fractionation in woody C_3 vegetation (resulting in more negative $\delta^{13}C$), although this has not been investigated in mixed C_3 and C_4 ecosystems (Diefendorf et al., 2010; Kohn 2010). Because the effect of MAP on soil $\delta^{13}C$ was positive, it is also unlikely that it reflects unaccounted patterns of OC or root allocation (Angelo & Pau, 2015). It is also possible that this relationship reflects increased abundance of C_4 NADP-me grasses that have less negative $\delta^{13}C$ (Cerling and Harris, 1999), although most likely this result is an artefact of low sample size. In contrast to soils, the strong link from C_4 relative cover abundance and bison $\delta^{13}C$ was only slightly improved by the addition of a SEM path from MAP, indicative of the stronger connection between herbaceous vegetation and herbivore diet at 100- km resolution. Working with bison data is potentially challenging because they have variable migratory routes (local to >100 km), sample vegetation across seasons, and they may consume herbs or shrubs (up to 2 %) or have dietary preferences, but may eat a substantial amount of sedges (Meagher, 1986; Coppedge et al., 1998). Our data suggest that despite these sources of variability, bison are strongly representative of the grass C_4 percentage at a coarse grain and are not systematically biased. Finally, given that the bison isotope data are up to 250 years older than the vegetation data (Fig. 5), the strong alignment of bison and vegetation data suggests an impressive degree of ecosystem and community level stasis in terms of relative representation of photosynthetic pathways in these grasslands.

One major difference between the bison and soil $\delta^{13}C$ data is the drastically different temporal and spatial scales at which they integrate C. Bison are mobile and sample grassland vegetation over large areas over short time scales (diet), whereas soils incorporate $\delta^{13}C$ variation across a local spatial range and over the time scale of soil carbon turnover. Our semivariogram analysis revealed that around one-third of variation in soil $\delta^{13}C$ is contained at local scales (here, <100 km)(Auerswald et al., 2009), suggesting that much of the unexplained variance in our statistical model predicting $\delta^{13}C$ is due to local variation not captured on our grid (Table 1). This contrasts with bison, which had much less unexplained local variation than the vegetation plot inventories, indicative of the coarse spatial grain over which these organisms integrate C.

In conclusion, across the North American Great Plains and in sites minimally impacted by land-use conversion, we found no systematic change in C_4 grass distributions over the last few hundred years. In particular, this result suggests that there has been no significant role for CO_2 fertilization of C_3 grasses at a biogeographic extent (Morgan et al., 2011; Cotton et al., 2016). To capture grass distributions at a broad extent during recent environmental change we used a multi-proxy approach that allowed us to assess the quality of isotopic proxies and examine differences in the spatial grains that different proxies represent. The spatial resolution of processes generating $\delta^{13}C$ heterogeneity should be thoroughly considered in determining the grain at which we analyse and make inferences from data (Goodchild, 2011). This means that different proxies will perform better than others when used to represent the broad spatial extents and coarse grain sizes over which ecologists and geologists often use them. We suggest that studies using $\delta^{13}C$ proxies explicitly address how well their isotopic proxies can be scaled-up (to larger grain sizes), especially when the spatial or temporal scale of C integration differs from the ecological processes in the study. One fruitful avenue for studies using stable isotope approaches would be to sample across gradients using a nested sampling scheme (e.g., using Modified-Whittaker plots; Stohlgren et al., 1998) to partition variation in soil $\delta^{13}C$ at different spatial ranges and to link that variation to processes at different spatial extents explicitly (e.g., variation driven by a rainfall gradient versus local soil heterogeneity). This work shows that bison $\delta^{13}C$ data are better vegetation proxies than soils at coarse resolutions. While soils and palaeosols may be useful for local-scale vegetation reconstructions, large-scale interpretations of palaeovegetation based on isotopic reconstructions should be made using grazers rather than soils. Ultimately, the reconstruction of post-industrial vegetation change reported here reveals surprisingly little variation in C_3 and C_4 grass relative abundance, in the face of massive global changes. This also implies that future changes in the C_3/C_4 composition of grasslands projected by biosphere models may be significantly overestimated.

ACKNOWLEDGMENTS

This project was funded by National Science Foundation award 1342703 to Christopher Still. NDS was funded by National Science Foundation award 1024535. Thank you to the reviewers who greatly improved this study.

REFERENCES

Angelo C.L. & Pau S. (2015) Root biomass and soil δ13C in C3 and C4 grasslands along a precipitation gradient. *Plant Ecology*, **216**, 615–627.

Asner G.P., Scurlock J.M., & A Hicke J. (2003) Global synthesis of leaf area index observations: implications for ecological and remote sensing studies. *Global Ecology and Biogeography*, **12**, 191–205.

Auerswald K., Wittmer M., Männel T.T., Bai Y.F., Schäufele R., & Schnyder H. (2009) Large regional-scale variation in C3/C4 distribution pattern of Inner Mongolia steppe is revealed by grazer wool carbon isotope composition. *Biogeosciences Discussions*, **6**, 545–574.

Ayliffe L.K., Cerling T. E., Robinson T., West A.G., Sponheimer M., Passey B. H., Hammer J., Roeder B., Dearing M.D., Ehleringer J.R. (2004) Turnover of carbon isotopes in tail hair and breath CO2 of horses fed an isotopically varied diet. *Oecologia,* 139: 11 – 22.

Bai E., Boutton T.W., Liu F., Wu X.B., Hallmark C.T., & Archer S.R. (2012) Spatial variation of soil δ13C and its relation to carbon input and soil texture in a subtropical lowland woodland. *Soil Biology and Biochemistry*, **44**, 102–112.

Beerling D.J. & Royer D.L. (2011) Convergent cenozoic CO2 history. *Nature Geoscience*, **4**, 418–420.

Blunden J. & Arndt D.S. (2016) State of the Climate in 2015. *Bulletin of the American Meteorological Society*, **97**, Si-S275.

Bond W.J. & Midgley G.F. (2012) Carbon dioxide and the uneasy interactions of trees and savannah grasses. *Philosophical Transactions of the Royal Society B: Biological Sciences*, **367**, 601–612.

Bowen G.J. (2010) Isoscapes: Spatial Pattern in Isotopic Biogeochemistry. *Annual Review of Earth and Planetary Sciences*, **38**, 161–187.

519 Bowling D.R., Pataki D.E., & Randerson J.T. (2008) Carbon isotopes in terrestrial ecosystem
520 pools and CO_2 fluxes. *New Phytologist*, **178**, 24–40.

521 Cerling T.E., Harris J.M., MacFadden B.J., Leakey M.G., Quade J., Eisenmann V., & Ehleringer
522 J.R. (1997) Global vegetation change through the Miocene/Pliocene boundary. *Nature*,
523 **389**, 153–158.

524 Cerling T.E., & Harris J.M.. (1999) Carbon Isotope Fractionation between Diet and Bioapatite in
525 Ungulate Mammals and Implications for Ecological and Paleoecological Studies.
526 *Oecologia* 120: 347–63
527
528 Cerling T.E., Wynn J.G., Andanje S.A., Bird M.I., Korir D.K., Levin N.E., Mace W., Macharia
529 A.N., Quade J., & Remien C.H. (2011) Woody cover and hominin environments in the
530 past 6 million years. *Nature*, **476**, 51–56.

531 Chen S.T., Smith S.Y., Sheldon N.D., & Strömberg C.A.E. (2015) Regional-scale variability in
532 the spread of grasslands in the late Miocene. *Palaeogeography, Palaeoclimatology,*
533 *Palaeoecology*, **437**, 42–52.

534 Coppedge, Bryan R., David M. Leslie Jr, and James H. Shaw. (1998) Botanical composition of
535 bison diets on tallgrass prairie in Oklahoma. *Journal of Range Management*, 379-382.

536 Collatz G.J., Berry J.A., & Clark J.S. (1998) Effects of climate and atmospheric CO_2 partial
537 pressure on the global distribution of C_4 grasses: present, past, and future. *Oecologia*,
538 **114**, 441–454.

539 Cotton J.M., Cerling T.E., Hoppe K.A., Mosier T.M., & Still C.J. (2016) Climate, CO2, and the
540 history of North American grasses since the Last Glacial Maximum. *Science Advances*, **2**,
541 e1501346–e1501346.

542 Cotton J.M. & Sheldon N.D. (2012) New constraints on using paleosols to reconstruct
543 atmospheric pCO2. *Geological Society of America Bulletin*, **124**, 1411–1423.

544 Dawson T.E., Mambelli S., Plamboeck A.H., Templer P.H., & Tu K.P. (2002) Stable Isotopes in
545 Plant Ecology. *Annual Review of Ecology and Systematics*, **33**, 507–559.

546 Diefendorf A.F., Mueller K.E., Wing S.L., Koch P.L., & Freeman K.H. (2010) Global patterns in
547 leaf 13C discrimination and implications for studies of past and future climate.
548 *Proceedings of the National Academy of Sciences*, **107**, 5738–5743.

549 Dunn R.E., Stromberg C.A.E., Madden R.H., Kohn M.J., & Carlini A.A. (2015) Linked canopy,
550 climate, and faunal change in the Cenozoic of Patagonia. *Science*, **347**, 258–261.

551 Ehleringer J.R., Buchmann N., & Flanagan L.B. (2000) Carbon isotope ratios in belowground
552 carbon cycle processes. *Ecological Applications*, **10**, 412–422.

553 Ehleringer J.R., Cerling T.E., & Helliker B.R. (1997) C_4 photosynthesis, atmospheric CO_2, and
554 climate. *Oecologia*, **112**, 285–299.

555 Farquhar G.D., Ehleringer J.R., & Hubick K.T. (1989) Carbon isotope discrimination and
556 photosynthesis. *Annual review of plant biology*, **40**, 503–537.

557 von Fischer J.C., Tieszen L.L., & Schimel D.S. (2008) Climate controls on C_3 vs. C_4
558 productivity in North American grasslands from carbon isotope composition of soil
559 organic matter. *Global Change Biology*, **14**, 1141–1155.

560 Fox D.L. & Koch P.L. (2003) Tertiary history of C4 biomass in the Great Plains, USA. *Geology*,
561 **31**, 809.

562 Friedli H., Lötscher H., Oeschger H., Siegenthaler U., Stauffer B. (1986) Ice core record of the
563 13C/12C ratio of atmospheric CO2 in the past two centuries. *Nature*, 324: 237 – 238.
564
565 Gadbury C., Todd L.C., Jahren A.H., Amundson R. (2000) Spatial and temporal variations in the
566 isotopic composition of bison tooth enamel from the Early Holocene Hudson – Meng
567 Bone Bed, Nebraska. *Palaeogeogr. Palaeoclimatol. Palaeoecol*, 157: 79 – 93.
568
569 Goodchild M.F. (2011) Scale in GIS: An overview. *Geomorphology*, **130**, 5–9.

570 Grace J.B., Anderson T.M., Olff H., & Scheiner S.M. (2010) On the specification of structural
571 equation models for ecological systems. *Ecological Monographs*, **80**, 67–87.

572 Grace J.B., Smith M.D., Grace S.L., Collins S.L., & Stohlgren T.J. (2000) Interactions between
573 fire and invasive plants in temperate grasslands of North America. 40–65.

574 Grass Phylogeny Working Group II (2012) New grass phylogeny resolves deep evolutionary
575 relationships and discovers C4 origins. *New Phytologist*, **193**, 304–312.

576 Griffith D.M., Anderson T.M., Osborne C.P., Strömberg C.A.E., Forrestel E.J., & Still C.J.
577 (2015) Biogeographically distinct controls on C_3 and C_4 grass distributions: merging
578 community and physiological ecology: Climate disequilibrium in C_4 grass distributions.
579 *Global Ecology and Biogeography*, **24**, 304–313.

580 Heckathorn S.A., McNaughton S.J., & Coleman J.S. (1999) C_4 Plants and Herbivory. *C4 Plant*
581 *Biology* pp. 285–312. Academic Press, San Diego.

582 Hobson K.A. (1999) Tracing origins and migration of wildlife using stable isotopes: a review.
583 *Oecologia*, **120**, 314–326.

584 Hobson K.A., Møller A.P., & Van Wilgenburg S.L. (2012) A multi-isotope (δ13C, δ15N, δ2H)
585 approach to connecting European breeding and African wintering populations of barn
586 swallow (Hirundo rustica). *Animal Migration*, **1**, .

587 Hoppe K.A., Paytan A., & Chamberlain P. (2006) Reconstructing grassland vegetation and
588 paleotemperatures using carbon isotope ratios of bison tooth enamel. *Geology*, **34**, 649–
589 652.

590 Jenkins D.G. & Ricklefs R.E. (2011) Biogeography and ecology: two views of one world.
591 *Philosophical Transactions of the Royal Society B: Biological Sciences*, **366**, 2331–2335.

592 Keeling C.D., Piper S.C., Bacastow R.B., Wahlen M., Whorf T.P., Heimann M., Meijer H.A.
593 (2005) Atmospheric CO2 and 13CO2 exchange with the terrestrial biosphere and oceans
594 from 1978 to 2000: Observations and carbon cycle implications, in A History of
595 Atmospheric CO2 and Its Effects on Plants, Animals, and Ecosystems, J. R. Ehleringer,
596 T. E. Cerling, M. D. Dearing, Eds. (Springer-Verlag, New York), pp. 83 – 113.

Kaplan J.O., Prentice I.C., & Buchmann N. (2002) The stable carbon isotope composition of the terrestrial biosphere: Modeling at scales from the leaf to the globe: CARBON ISOTOPE COMPOSITION OF THE TERRESTRIAL BIOSPHERE. *Global Biogeochemical Cycles*, **16**, 8-1-8–11.

Kohn M.J.,& Fremd T.J. (2008) Miocene Tectonics and Climate Forcing of Biodiversity, Western United States. *Geology* 36: 783.

Kohn M.J. (2010) Carbon isotope compositions of terrestrial C3 plants as indicators of (paleo) ecology and (paleo) climate. *Proceedings of the National Academy of Sciences*, **107**, 19691–19695.

Kohn, M.J. & McKay M.P. (2012) Paleoecology of Late Pleistocene–Holocene Faunas of Eastern and Central Wyoming, USA, with Implications for LGM Climate Models. *Palaeogeography, Palaeoclimatology, Palaeoecology*, 326–328: 42–53.

Ladd B., Peri P.L., Pepper D.A., Silva L.C.R., Sheil D., Bonser S.P., Laffan S.W., Amelung W., Ekblad A., Eliasson P., Bahamonde H., Duarte-Guardia S., & Bird M. (2014) Carbon isotopic signatures of soil organic matter correlate with leaf area index across woody biomes. *Journal of Ecology*, **102**, 1606–1611.

Leavitt S.W., Follett R.F., Kimble J.M., & Pruessner E.G. (2007) Radiocarbon and δ13C depth profiles of soil organic carbon in the U.S. Great Plains: A possible spatial record of paleoenvironment and paleovegetation. *Quaternary International*, **162**–**163**, 21–34.

Liang L.L., Riveros-Iregui D.A., & Risk D.A. (2016) Spatial and seasonal variabilities of the stable carbon isotope composition of soil CO_2 concentration and flux in complex terrain: Variability of the $\delta^{13}C$ in Soil CO_2. *Journal of Geophysical Research: Biogeosciences*, .

Long S.P. (1999) Environmental Responses. *C4 plant biology* pp. 313–373. Academic Press, San Diego.

Lüthi D., Le Floch M., Bereiter B., Blunier T., Barnola J.M., Siegenthaler U., Raynaud, J.D. Jouzel, Fischer H., Kawamura K., Stocker T. (2008) High-resolution carbon dioxide concentration record 650,000–800,000 years before present. *Nature* **453**, 379–382

MacKenzie K.M., Palmer M.R., Moore A., Ibbotson A.T., Beaumont W.R.C., Poulter D.J.S., & Trueman C.N. (2011) Locations of marine animals revealed by carbon isotopes. *Scientific Reports*, **1**, .

Meagher, M. (1989) Range Expansion by Bison of Yellowstone National Park. *Journal of Mammalogy* 70: 670–75.

Morgan J.A., LeCain D.R., Pendall E., Blumenthal D.M., Kimball B.A., Carrillo Y., Williams D.G., Heisler-White J., Dijkstra F.A., & West M. (2011) C4 grasses prosper as carbon dioxide eliminates desiccation in warmed semi-arid grassland. *Nature*, **476**, 202–205.

Nachtergaele F. & Batjes N. (2012) *Harmonized world soil database.* FAO,

Osborne C.P., Salomaa A., Kluyver T.A., Visser V., Kellogg E.A., Morrone O., Vorontsova M.S., Clayton W.D., & Simpson D.A. (2014) A global database of C $_4$ photosynthesis in grasses. *New Phytologist*, **204**, 441–446.

Paruelo J.M. & Lauenroth W.K. (1996) Relative Abundance of Plant Functional Types in Grasslands and Shrublands of North America. *Ecological Applications*, 6: 1212–24.

Passey B.H., Cerling T.E., Perkins M.E., Voorhies M.R., Harris J.M., & Tucker S.T. (2002) Environmental change in the Great Plains: an isotopic record from fossil horses. *The Journal of Geology*, **110**, 123–140.

Powell R.L., Yoo E.-H., & Still C.J. (2012) Vegetation and soil carbon-13 isoscapes for South America: integrating remote sensing and ecosystem isotope measurements. *Ecosphere*, **3**, 1–25.

Power M.J. et al. (2008) Changes in Fire Regimes since the Last Glacial Maximum: An Assessment Based on a Global Synthesis and Analysis of Charcoal Data. *Climate Dynamics* 30: 887–907.

R Development Core Team (2012) *R: A Language and Environment for Statistical Computing*. R Development Core Team,

Ramankutty N. & Foley J.A. (1999) Estimating historical changes in global land cover: Croplands from 1700 to 1992. *Global Biogeochemical Cycles*, **13**, 997–1027.

Ripple W.J., Beschta R.L., & Painter L.E. (2015) Trophic cascades from wolves to alders in Yellowstone. *Forest Ecology and Management*, **354**, 254–260.

Rosseel Y. (2012) lavaan: An R package for structural equation modeling. *Journal of Statistical Software*, **48**, 1–36.

Sage R.F., Christin P.A., & Edwards E.J. (2011) The C4 plant lineages of planet Earth. *Journal of Experimental Botany*, **62**, 3155–3169.

Sage R.F. & Sultmanis S. (2016) Why Are There No C4 Forests? *Journal of Plant Physiology*, .

Scheiter S., Higgins S.I., Osborne C.P., Bradshaw C., Lunt D., Ripley B.S., Taylor L.L., & Beerling D.J. (2012) Fire and fire-adapted vegetation promoted C_4 expansion in the late Miocene. *New Phytologist*, **195**, 653–666.

Segers J.L. & Broders H.G. (2015) Carbon (δ13C) and Nitrogen (δ15N) Stable Isotope Signatures in Bat Fur Indicate Swarming Sites Have Catchment Areas for Bats from Different Summering Areas. *PLOS ONE*, **10**, e0125755.

Sexton J.O., Song X.-P., Feng M., Noojipady P., Anand A., Huang C., Kim D.-H., Collins K.M., Channan S., DiMiceli C., & Townshend J.R. (2013) Global, 30-m resolution continuous fields of tree cover: Landsat-based rescaling of MODIS vegetation continuous fields with lidar-based estimates of error. *International Journal of Digital Earth*, **6**, 427–448.

Still C.J., Berry J.A., Collatz G.J., & DeFries R.S. (2003) Global distribution of C_3 and C_4 vegetation: Carbon cycle implications. *Global Biogeochemical Cycles*, **17**, 1006.

674 Stohlgren T.J., Bull K.A., & Otsuki Y. (1998) Comparison of rangeland vegetation sampling
675 techniques in the Central Grasslands. *Journal of range management*, **51**, 164–172.

676 Strömberg C. (2011) Evolution of Grasses and Grassland Ecosystems. *Annual Review of Earth*
677 *and Planetary Sciences*, **39**, 517–544.

678 Teeri J.A. & Stowe L.G. (1976) Climatic patterns and the distribution of C_4 grasses in North
679 America. *Oecologia*, **23**, 1–12.

680 Tieszen L.L. (1994) Stable isotopes on the Plains: Vegetation analyses and diet determinations.
681 Skeletal Biology in the Great Plains: A Multidisciplinary View, D. W. Owsley, R. L.
682 Jantz, Eds. (Smithsonian Press, Washington, DC), pp. 261 – 282.
683
684 Tilman D. & Wedin D. (1991) Dynamics of Nitrogen Competition Between Successional
685 Grasses. *Ecology*, **72**, 1038–1049.

686 Tipple B.J., Meyers S.R., & Pagani M. (2010) Carbon isotope ratio of Cenozoic CO_2 : A
687 comparative evaluation of available geochemical proxies: CENOZOIC $\delta^{13}C_{CO2}$.
688 *Paleoceanography*, **25**, .

689 Vitousek P.M., Aber J.D., Howarth R.W., Likens G.E., Matson P.A., Schindler D.W.,
690 Schlesinger W.H., & Tilman D.G. (1997) Technical Report: Human Alteration of the
691 Global Nitrogen Cycle: Sources and Consequences. *Ecological Applications*, **7**, 737.

692 Widga C.J., Walker D., & Stockli L.D. (2010) Middle Holocene Bison Diet and Mobility in the
693 Eastern Great Plains (USA) Based on δ 13C, δ 18O, and 87Sr/86Sr Analyses of Tooth
694 Enamel Carbonate. *Quaternary Research* 73: 449–63.

695 Winslow J.C., Hunt E.R., & Piper S.C. (2003) The influence of seasonal water availability on
696 global C_3 versus C_4 grassland biomass and its implications for climate change research.
697 *Ecological Modelling*, **163**, 153–173.

698 Wood S. & Wood M.S. (2016) Package "mgcv." .

Wynn J.G. et al. (2006) Continental-Scale Measurement of the Soil Organic Carbon Pool with Climatic, Edaphic, and Biotic Controls. *Global Biogeochemical Cycles*, 20: 2-12

Wynn J.G. & Bird M.I. (2007) C4-derived soil organic carbon decomposes faster than its C3 counterpart in mixed C3/C4 soils. *Global Change Biology*, **13**, 2206–2217.

SUPPORTING INFORMATION

Additional Supporting Information may be found in the online version of this article:

Appendix S1. Supplemental methods for sampling scale optimization, C_3/C_4 mixing model, temporal analysis, and SEM in addition to raw data for soils, data access information, and gridded data.

BIOSKETCH

Daniel M. Griffith conducts research focused on the biogeography of grasses and the ecology of savanna and grassland ecosystems.

Author contributions: D.M.G. conducted the data analyses and drafted the manuscript. All authors were involved in idea generation, data collection, and editing.

Editor: Pablo Vargas

TABLES

Table 1. Fitted semivariogram results for North American plot, soil, and bison data. Nugget variance reflects the amount of variation present at scales below the grain size of the data (i.e., 100 km^2 grid cells) and non-spatial measurement error. The sill represents the total variance of the data. Therefore, the proportion of variation unaccounted for at fine resolutions can be assessed by dividing the Nugget variance by the Sill

Variable	Nugget variance	Sill	Range	Nugget / Sill

			(km)	(%)
C_4 Cover (%)	0.02	0.09	1272	19.3
Soil $\delta^{13}C$ (‰)	2.05	6.59	878	31.1
Bison $\delta^{13}C$ (‰)	0.56	6.86	536	8.2

FIGURE LEGENDS

Figure 1. Vegetation plot grass percentage C_4 cover (A), soil $\delta^{13}C$ (B), and bison $\delta^{13}C$ (C) data from North America resampled onto a common 100-km grid. Raster cells shown for isotope data only when they overlap with plot data, and vice versa.

Figure 2. A: Surface soil $\delta^{13}C$ as a function of grass percentage C_4 cover in North American vegetation plots. B: Bison $\delta^{13}C$ as a function of vegetation C_4 cover; these data have been adjusted to account for tissue fractionation and represent the presumptive dietary $\delta^{13}C$ of bison under preindustrial atmospheric conditions. Trend lines and grey-shaded 95% prediction intervals are from weighted least squares regression models.

Figure 3. *A priori* conceptual models relating environmental and biotic factors to variation in soil $\delta^{13}C$ (A) and bison $\delta^{13}C$ (B) in North America. SEM analyses were conducted using these models as starting points. Details about model selection procedure and the individual paths can be found in the main text. OC is soil organic carbon.

Figure 4. Final structural equation models, relating environmental and biotic factors to variation in North American soil $\delta^{13}C$ (A) and bison $\delta^{13}C$ (B), showing significant paths (Supplementary Methods). Path coefficients for direct effects are represented by arrows that are either significantly positive (solid lines) or negative (dashed). Arrow widths are proportional to the standardized effect sizes. Response variables have small text boxes in the top right showing the r^2 values for their respective linear sub-models.

Figure 5. Residual variation in animal diet $\delta^{13}C$ (from a linear model with 50 years of diet $\delta^{13}C$ data as a function of C_4 cover), for modern, historical, and fossil tissues over log-time. As such, data points represent deviations of diet $\delta^{13}C$ from modern vegetation abundance—positive means higher values than current vegetation. The black dotted line is a residual of zero. The vertical grey lines mark the boundaries between the modern animal samples used in our analysis and historical (50 yr) or fossil data (300 yr) from Cotton et al. (2016) that are not otherwise reported in this study. Fossil samples are radiocarbon dated, but the modern samples were directly dated based on registration as museum specimen; all dates were converted to years before 2016 CE (Years BP) to fit on the same axis. The smoothed grey line is a GAM fit with 95% confidence intervals (grey polygon). The GAM represents the relationship between the $\delta^{13}C$ residuals and time. The mean residuals ± CI overlap zero (i.e., no change) for all modern and historical time-points supporting the assertion that C_4 abundance has not changed much over the last 300 years in North America. Fossil data are shown as a reference in order to illustrate the relative stasis in composition of the modern and historical data, and the drivers of fossil variation are discussed in Cotton et al. (2016). The fossil bison $\delta^{13}C$ values used have also been adjusted to account for the pre-industrial atmospheric $\delta^{13}C$. The second axis and the grey dotted line represent atmospheric CO_2 change.

FIGURES

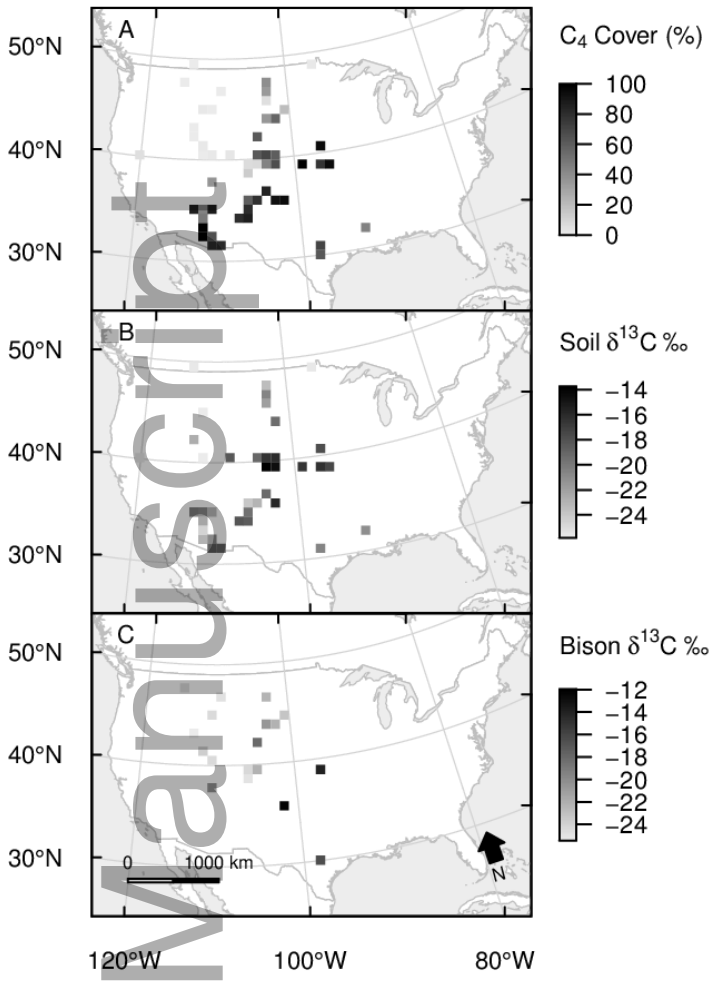

783

784 **Figure 1.**

785

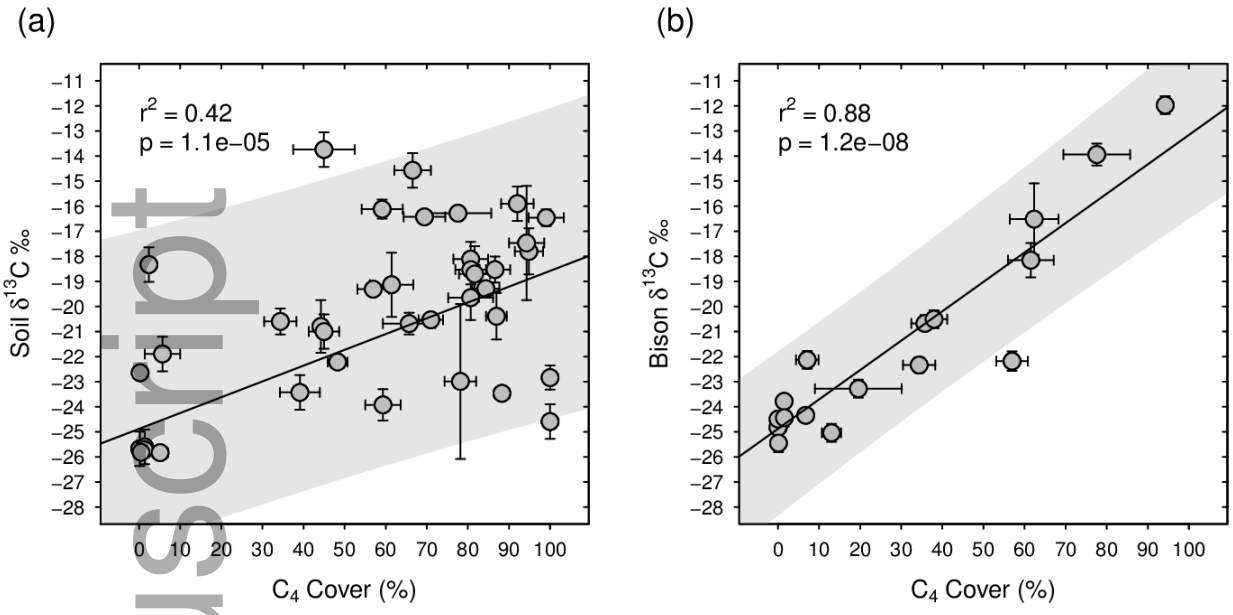

Figure 2.

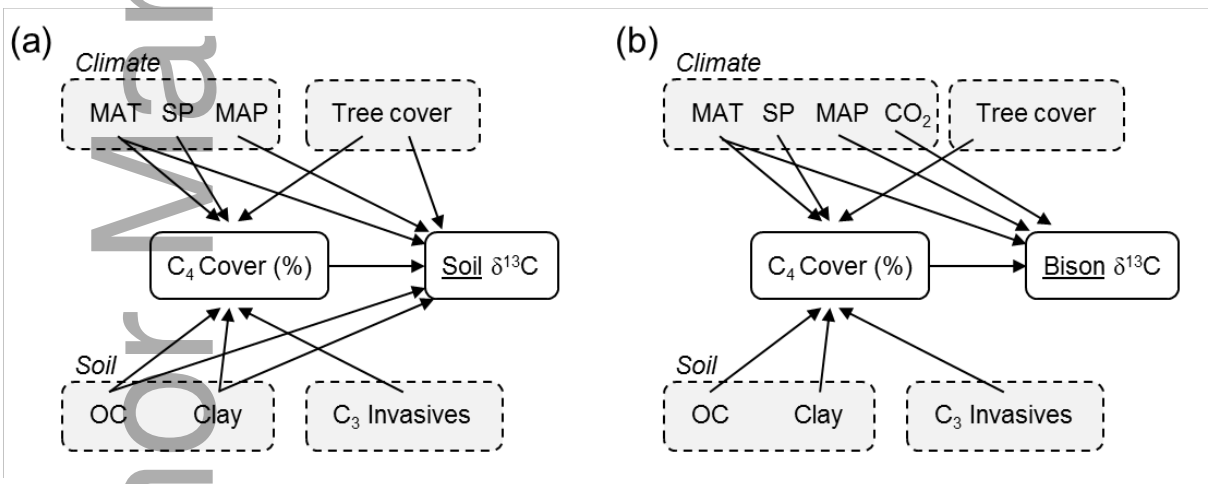

Figure 3.

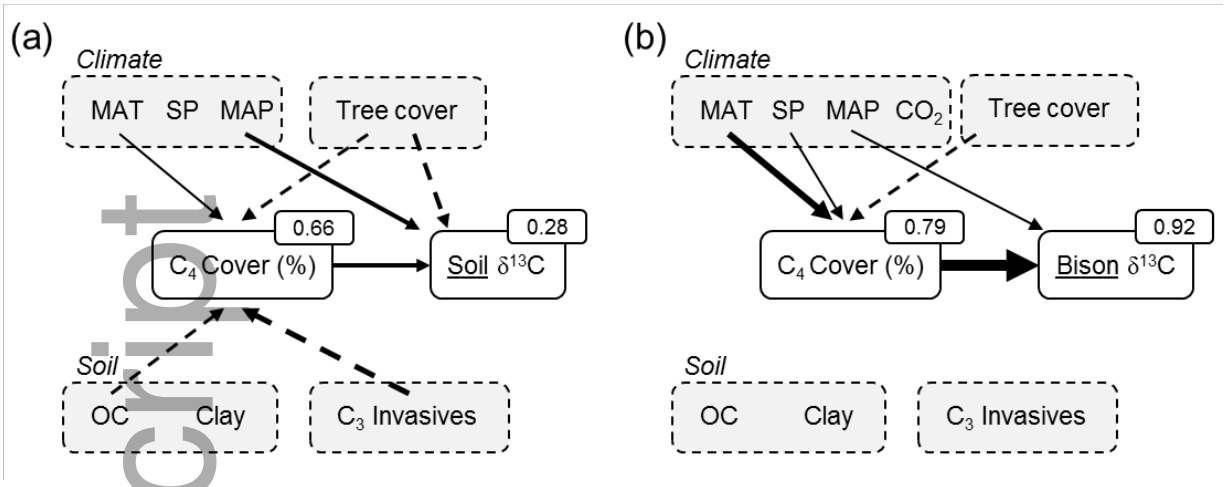

792
793 **Figure 4.**

794

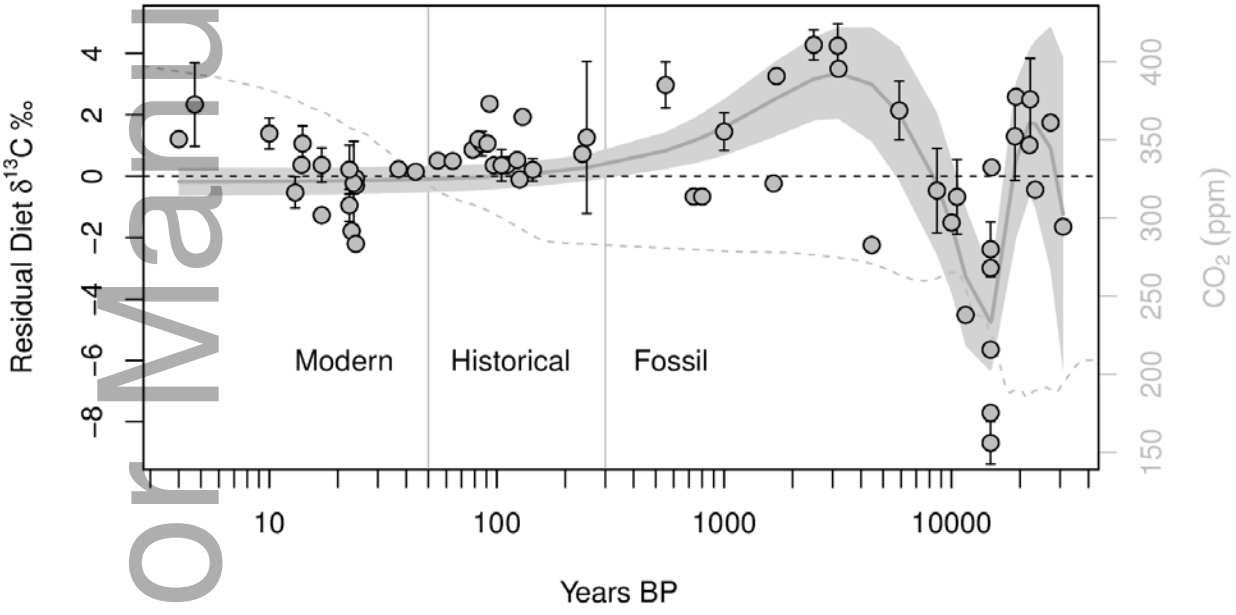

795
796 **Figure 5.**

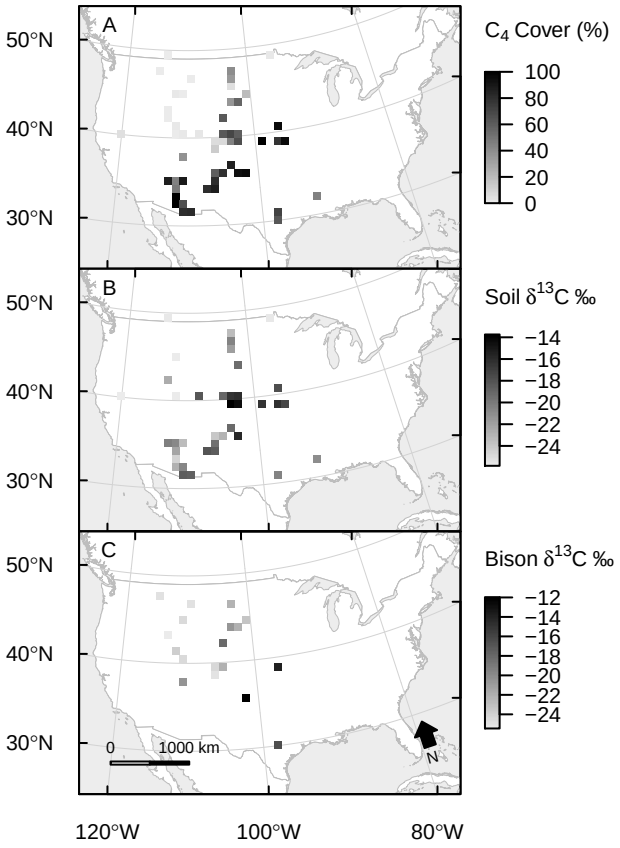

jbi_13061_f1.eps

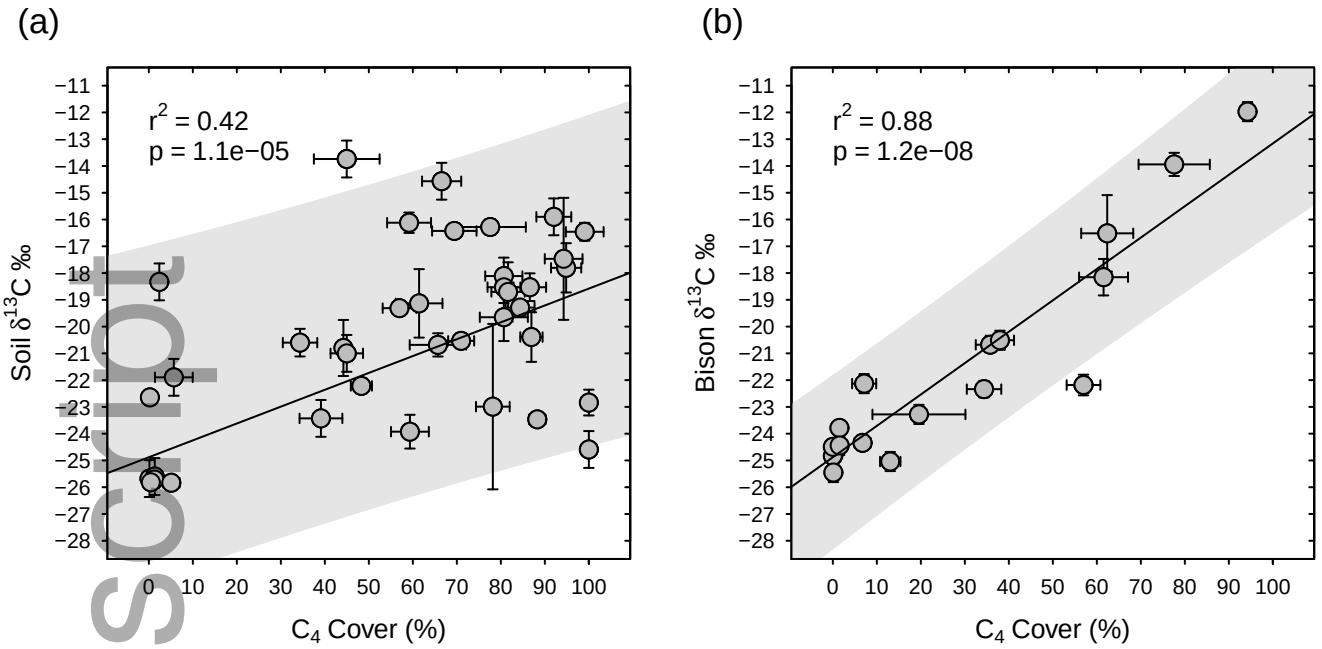

jbi_13061_f2.eps

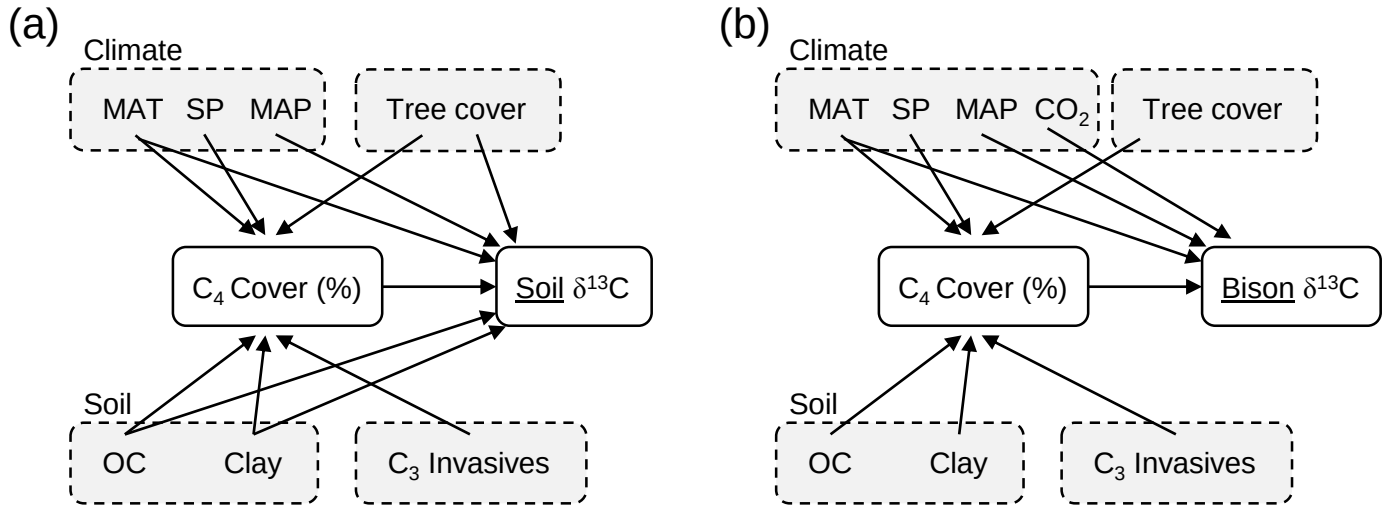

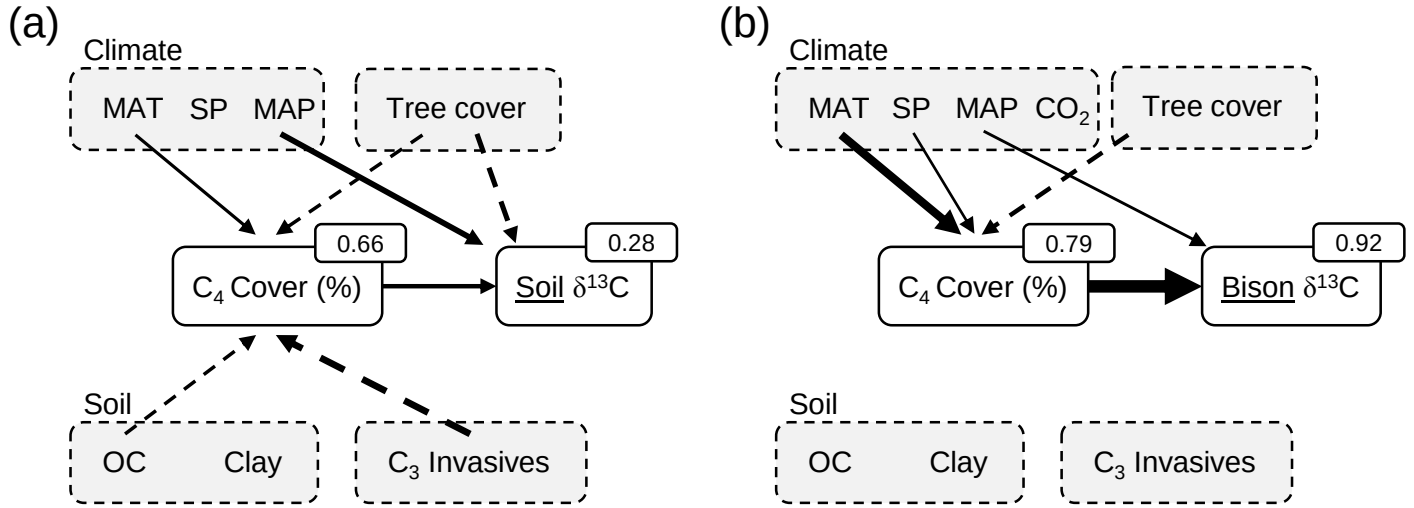

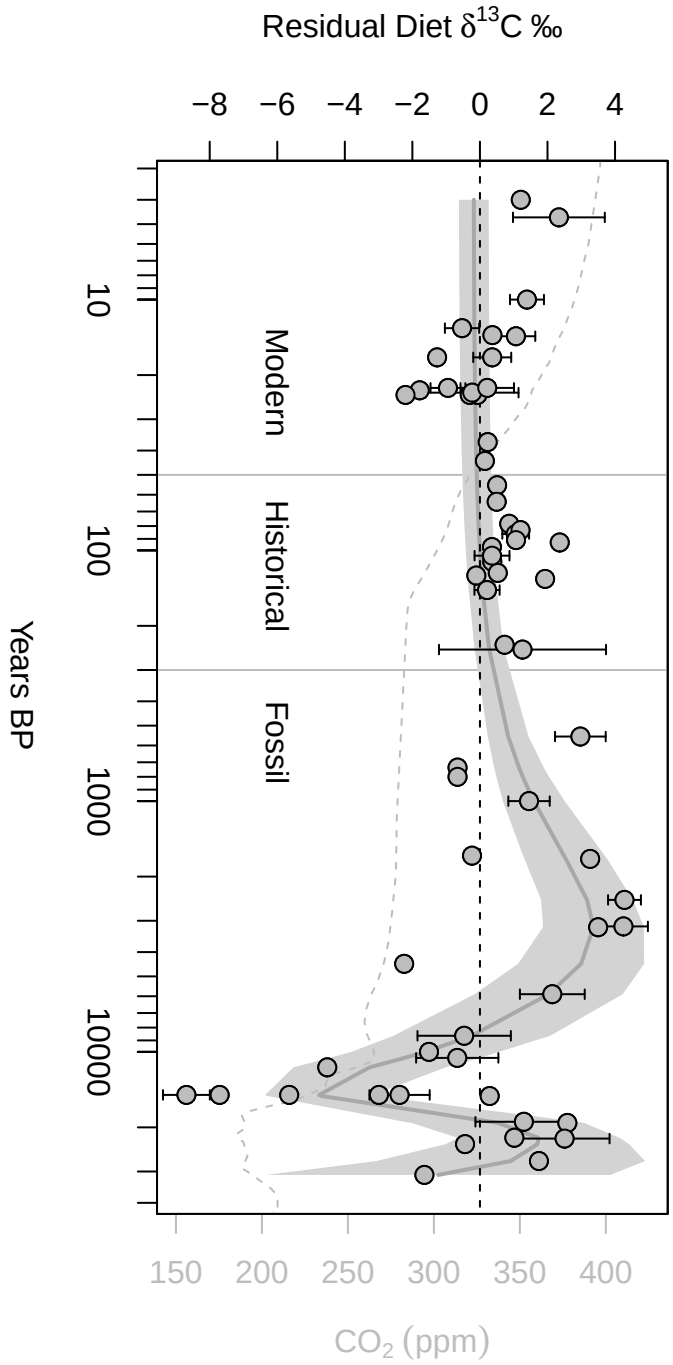

jbi_13061_f5.eps